Condensate in quasi-two-dimensional turbulence

S. Musacchio

Department of Physics, University of Torino, via P. Giuria 1, 10125 Torino, Italy

G. Boffetta

Department of Physics and INFN, University of Torino, via P. Giuria 1, 10125 Torino, Italy

We investigate the process of formation of large-scale structures in a turbulent flow confined in a thin layer. By means of direct numerical simulations of the Navier-Stokes equations, forced at an intermediate scale L_f, we obtain a split of the energy cascade in which one fraction of the input goes to small scales generating the three-dimensional direct cascade. The remaining energy flows to large scales producing the inverse cascade which eventually causes the formation of a quasi-two-dimensional condensed state at the largest horizontal scale. Our results show that the connection between the two actors of the split energy cascade in thin layers is tighter than what was established before: the small-scale three-dimensional turbulence acts as an effective viscosity and dissipates the large-scale energy thus providing a viscosity-independent mechanism for arresting the growth of the condensate. This scenario is supported by quantitative predictions of the saturation energy in the condensate.

In many instances, geophysical and astrophysical flows are confined in thin layers of small aspect ratio either by material boundaries or by other physical mechanisms which constrain the motion. The thickness of such layers can be much smaller than the typical horizontal scales, while being at the same time much larger than the dissipative viscous scales. Turbulent flows in such quasi-two-dimensional (2D) geometries display an interesting phenomenology with both 2D and three-dimensional (3D) features. Numerical [1–4] and experimental [5–8] works have demonstrated the emergence of a *split energy cascade* in which a fraction of the energy flow to large scales (as in a pure 2D flow) and the remaining part goes to small scales producing the 3D direct cascade. The key parameter which controls the relative flux of the two energy cascades is the geometric ratio $S = L_z/L_f$ between the confining scale L_z and the forcing scale L_f [1,2]. In particular, it has been shown that there exists a critical ratio S^* above which the inverse cascade is suppressed and the thin layer recovers the usual 3D phenomenology [2,9]. In the limit $S \to 0$, when the thickness becomes smaller than the viscous scale, vertical motion is suppressed and the flow fully recovers the 2D phenomenology.

The bidimensionalization of the flow, and in particular the value of S^*, is affected by other physical factors, besides confinement. Rotation along the confined direction z in general favors the bidimensionalization, increasing the relative intensity of the inverse flux at given S with respect to the nonrotating case [10–13]. Conversely, a stable stratification of the density produces an increase of the effective dimensionality of the flow and suppresses the large-scale energy transfer [14,15].

The inverse energy cascade generates a very long, nonstationary transient with an increasing value of kinetic energy of the flow. A fraction of the energy injected at scale L_f goes to the large scales where it is not dissipated by viscosity and, for finite horizontal extensions, accumulates producing a large-scale vortex system called the *condensate* [16,17]. The statistics of the condensate

has been investigated in detail by experiments [8,18–20] and numerical simulations [21–25] in the 2D limit $S = 0$. In the case of a square box with periodic boundary conditions, the condensate is a pair of system-size vortices of opposite sign. The vorticity profile of these vortices has been shown to display universal features, independent of the forcing mechanism which produces the inverse cascade [21,23]. Changing the shape of the domain from square to rectangular, the emergence of jets in the condensed state with a complex phenomenology has also been observed [25,26].

The growth of the energy of the condensate can be arrested by different mechanisms. The presence of a linear friction force $\alpha\boldsymbol{u}$ (as in Refs. [23–25]) causes the saturation of the energy to the value $E_c \simeq \varepsilon_{\text{inv}}/2\alpha$, where ε_{inv} is the flux of the inverse cascade. Further, in the case in which the forcing is correlated in time, it has been shown that the fast sweeping due to the large-scale velocity decorrelates the forcing and the velocity field. As a consequence, the energy input rate vanishes at long times causing the saturation of the condensate [22]. Even in the absence of a friction force and in the ideal case of a forcing which guarantees a constant energy input (as in the case of random-in-time forcing), any finite viscosity will eventually produce a sink of energy at large scales, thus arresting the growth of the condensate at finite energy. In this case, the value of the asymptotic energy E_c is determined by the balance between the flux of the inverse cascade ε_{inv} and the viscous dissipation at the scale of the condensate L, $\varepsilon_{\text{inv}} \simeq 2\nu E_c/L^2$, which gives the dimensional predictions $E_c \sim \varepsilon_{\text{inv}}L^2/\nu$ [27]. Estimating the time required to reach the steady state as $t_c \simeq E_c/\varepsilon_{\text{inv}}$ one gets $t_c \sim L^2/\nu$ [27]. In the limit of very large Reynolds number Re, equivalent to vanishing viscosity (which is relevant for geophysical applications), the flux of the inverse cascade becomes independent of the small-scale viscosity [28], and therefore the asymptotic energy of the condensate grows without limits (i.e., $E_c, t_c \to \infty$ as $\nu \to 0$).

In this Rapid Communication we show that this divergence is removed when a thin layer, with finite S, is considered. The direct energy cascade at scales below L_f produces a small-scale 3D flow which acts as an effective eddy viscosity which, in the large Re limit, becomes independent of the value of the molecular viscosity. This eddy viscosity arrests the condensate at an energy level much smaller than that obtained by the dimensional estimate $E_c \sim \varepsilon_{\text{inv}}L^2/\nu$.

To investigate quantitatively this prediction, we performed a set of direct numerical simulations of the 3D Navier-Stokes equation for an incompressible velocity field $\boldsymbol{u}(\boldsymbol{x}, t)$ (with $\nabla \cdot \boldsymbol{u} = 0$)

$$\frac{\partial \boldsymbol{u}}{\partial t} + \boldsymbol{u} \cdot \nabla \boldsymbol{u} = -\nabla p + \nu \nabla^2 \boldsymbol{u} + \boldsymbol{f}, \tag{1}$$

where the constant density has been adsorbed into the pressure p and ν is the kinematic viscosity. The two-dimensional forcing $\boldsymbol{f}$ is restricted to the two horizontal components (2D2C) $\boldsymbol{f}(\boldsymbol{x}) = [f_x(x, y), f_y(x, y), 0]$. It is Gaussian, white in time and in Fourier space is confined in a narrow cylindrical shell of wave numbers centered around $K_f = 2\pi/L_f$. Thanks to the delta correlation in time, the rates of injection of energy ε and of enstrophy $\beta = K_f^2\varepsilon$ do not depend on the flow, and they are kept fixed. Simulations are performed in a triply periodic domain with horizontal sizes $L_x = L_y = 2\pi$ and aspect ratio $r = L_x/L_z$, by means of a fully parallel, fully dealiased pseudospectral code with a second-order Runge-Kutta time stepping and explicit integration of the linear part. The resolution is $N_x = N_y = rN_z = 1024$ with uniform grid for two aspect ratios $r = 32$ and $r = 64$. The wave number of the forcing is fixed at $K_f = 8$. The characteristic time and kinetic energy at the forcing scale are defined as $t_f = \beta^{-1/3}$ and $E_f = \varepsilon t_f$.

Simulations of the split cascade in a thin layer are very demanding numerically since their need to resolve phenomena at very different scales: the horizontal box (of size $L_x = L_y$) must be much larger than the forcing scale L_f for the development of the inverse cascade which also requires $L_f > L_z$ [2]. Finally, scale separation between L_z and the viscous scale $\eta = (\varepsilon^3/\nu)^{1/4}$ is needed to produce the direct energy cascade. Therefore, to increase the extension of the direct inertial range, the viscous term in Eq. (1) is replaced by a hyperviscous term $(-1)^{p-1}\nu_p\nabla^{2p}\boldsymbol{u}$ with $p = 8$ and $\nu_p = 10^{-37}$. We do not use any large-scale dissipation (such as linear friction).

At $t = 0$, the velocity field is initialized to zero plus a small random perturbation, which triggers the 3D instability. The energy of the initial perturbation is $E_{\text{pert}} \simeq 1.4 \times 10^{-7}E_f$. The total
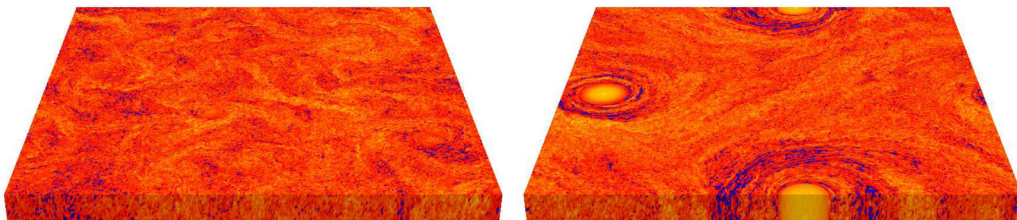
FIG. 1. Snapshots of the square vertical vorticity for the simulation at $S = 1/4$ at times $t = 24t_f$ (left panel) and $t = 1200t_f$ (right panel). The same logarithmic color scale is used for the two cases, with blue (yellow) representing small (large) values. For clarity, the vertical scale has been stretched by a factor 2.

simulation time is very long, in order to allow a complete development of the condensed state. In Fig. 1 we show two snapshots of the vertical component of the vorticity field $\boldsymbol{\omega} = \nabla \times \boldsymbol{u}$ at intermediate times and in the late stage of the simulation for $S = 1/4$. During the first stage of the evolution ($t = 24t_f$, left panel) the vorticity field is characterized by small-scale structures, with some organization induced by the large-scale velocity produced by the inverse cascade. The condensate becomes clearly visible at late times ($t = 1200t_f$, right panel). The vorticity field is dominated by a quasi-two-dimensional dipole, surrounded by small-scale three-dimensional turbulence. We observe that 3D structures are observable also inside the vortex structure.

In order to disentangle the 2D and 3D structures of the flow, following [3], we decompose the velocity field as $\boldsymbol{u} = \boldsymbol{u}^{2D} + \boldsymbol{u}^{3D}$. The 2D mode is defined in Fourier space as the mode $k_3 = 0$ of the horizontal velocity components $\hat{\boldsymbol{u}}^{2D}(k_1, k_2) = [\hat{u}_x(k_1, k_2), \hat{u}_y(k_1, k_2), 0]$. This corresponds to the average in physical space along the z direction. The 3D part is simply $\boldsymbol{u}^{3D} = \boldsymbol{u} - \boldsymbol{u}^{2D}$. The kinetic energy $E = (1/2)\langle|\boldsymbol{u}|^2\rangle = E^{2D} + E^{3D}$ is the sum of the two contributions $E^{2D} = (1/2)\langle|\boldsymbol{u}^{2D}|^2\rangle E^{3D} = (1/2)\langle|\boldsymbol{u}^{3D}|^2\rangle$. Here and in the following the brackets $\langle\cdots\rangle$ indicate the spatial average and we notice that the mixed term has zero average.

The temporal evolution of E^{2D} and E^{3D} is shown in Fig. 2. For short times we observe a linear growth of E^{2D}, which corresponds to the development of the inverse energy cascade. A linear fit of the growth rate dE^{2D}/dt for $50t_f < t < 250t_f$ provides an estimate of the flux ε_{inv} of the inverse cascade. We obtain $\varepsilon_{inv} = 0.65\varepsilon$ for $S = 1/8$ and $\varepsilon_{inv} = 0.41\varepsilon$ for $S = 1/4$. The dependence of the inverse energy flux on S is in agreement with previous numerical results [1,2]. At later times ($t > 3000t_f$ for $S = 1/8$ and $t > 2500t_f$ for $S = 1/4$) we observe the saturation of the energy to an almost constant value $E_c \simeq 800E_f$ for $S = 1/8$ and $E_c \simeq 320E_f$ for $S = 1/4$.

The energy of the 3D modes is much smaller than that of the 2D mode. It does not contribute significantly to the total energy. Its time evolution shows a first plateau at short times
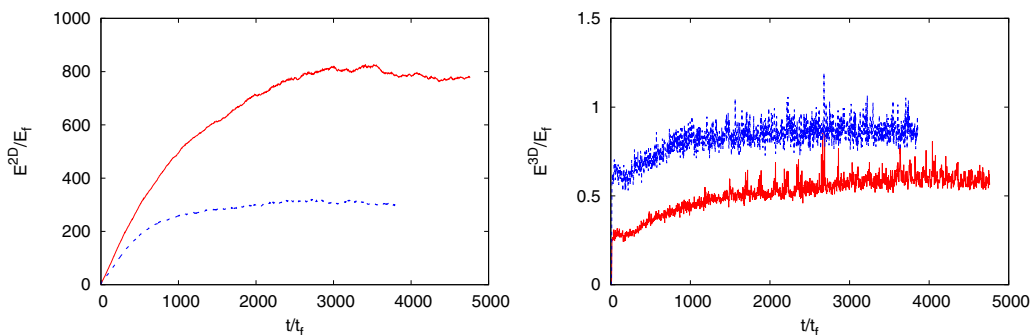

FIG. 2. Temporal evolution of the kinetic energy of the 2D mode E^{2D} (left panel) and E^{3D} (right panel) for $S = 1/8$ (red, solid line) and $S = 1/4$ (blue, dashed line).
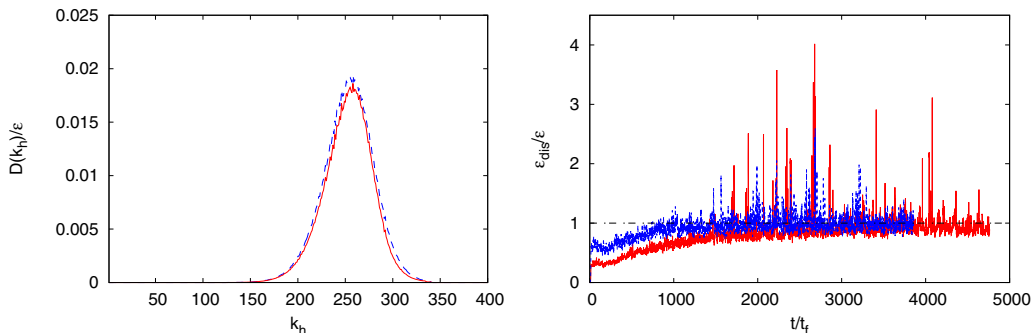
FIG. 3. Left: Dissipation spectra $D(k_h)$ as a function of $k_h = (k_x^2 + k_y^2)^{1/2}$ for $S = 1/8$ at time $t = 4050t_f$ (red, solid line), and for $S = 1/4$ at time $t = 2650t_f$ (blue, dashed line). Right: Temporal evolution of the energy dissipation rate ε_{dis} for $S = 1/8$ (red, solid line) and $S = 1/4$ (blue, dashed line).

($t < 200t_f$), with $E^{\text{3D}} \simeq 0.28 E_f$ for $S = 1/8$ and $E^{\text{3D}} \simeq 0.62 E_f$ for $S = 1/4$, which corresponds to the development of the direct energy cascade. After a slow growth, it reaches a second plateau with $E^{\text{3D}} \simeq 0.6 E_f$ for $S = 1/8$ and $E^{\text{3D}} \simeq 0.87 E_f$ for $S = 1/4$, As expected, the thicker layer $S = 1/4$ has smaller E^{2D} and higher E^{3D} than the thinner layer $S = 1/8$.

At variance with the case of 2D turbulence [27], the mechanism which arrests the growth of the condensate in the thin layer is not due to viscous effects at the scale of the condensate. A simple dimensional argument for the saturation of the energy due to hyperviscosity gives an estimate of the energy of the condensate $E_c^* \simeq \varepsilon_{\text{inv}}/K_x^{2p} \nu_p \simeq 10^{37} E_f$, which is many orders of magnitude higher than the observed value of E_c. This excludes the possibility that the saturation of kinetic energy is due to the hyperviscous dissipative forces at large scales. The dissipation spectrum, defined as

$$D(k_h) = \sum_{\substack{\boldsymbol{k} \\ k_x^2 + k_y^2 = k_h^2}} \nu_p |\boldsymbol{k}|^{2p} |\hat{\boldsymbol{u}}_{\boldsymbol{k}}|^2, \tag{2}$$

where $k_h = (k_1^2 + k_2^2)^{1/2}$ is the horizontal wave number, confirms that the hyperviscous dissipation is confined at high wave numbers and it does not affect directly the condensate (see Fig. 3, left panel).

Nonetheless, the saturation of the energy at long times can be achieved only if all the energy injected is dissipated at small scales, which is the only dissipative term in the equations. In Fig. 3 (right panel) we show the time series of the (hyper-)viscous energy dissipation rate $\varepsilon_{\text{dis}} = \langle 2(-1)^{p-1} \nu_p (\nabla^{2p} \mathbf{u}) \cdot \mathbf{u} \rangle$. After a rapid initial growth, energy dissipation displays a plateau for $20t_f < t < 250t_f$, with $\varepsilon_{\text{dis}} \simeq (0.32 \pm 0.02)\varepsilon$ for $S = 1/8$ and $\varepsilon_{\text{dis}} \simeq (0.58 \pm 0.02)\varepsilon$ for $S = 1/4$. Within the scenario of the split-energy cascade [3], the dissipation rate is equal to the flux of the direct energy cascade $\varepsilon_{\text{dir}} = \varepsilon - \varepsilon_{\text{inv}}$. The measured values of ε_{dis} are consistent with this picture. At long times, the large-scale 2D condensate interacts directly with the small-scale 3D flow, transferring its energy toward the 3D modes with $|\boldsymbol{k}| > k_z$ (at the rate ε_{inv}) where it is transported by the direct cascade to the dissipative scales. In this regime, which corresponds to the saturation of kinetic energy in Fig. 2, we therefore observe that ε_{dis} tends to values close to the energy input rate ε. We notice that for $t > 1000t_f$ the dissipation becomes extremely intermittent in time. This coupling between the large-scale condensate and small-scale 3D motion will be investigated in detail in the following.

In order to make quantitative predictions of the saturation energy of the condensate, we suppose that it is possible to model the 3D dynamics at scales $\ell < L_z$ and its interactions with the condensate by means of an effective eddy viscosity ν_{eddy}, which is much larger than the molecular (hyper) viscosity. Further, we assume that that the condensate reaches a steady state when the flux of the
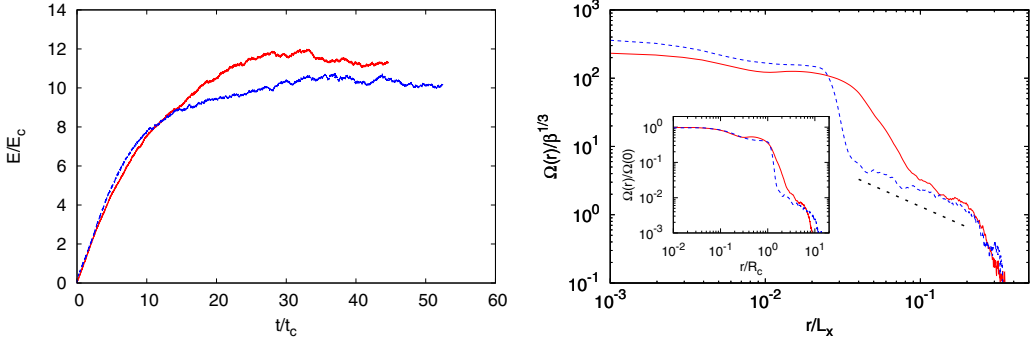
FIG. 4. Left: Temporal evolution of the kinetic energy rescaled with E_c and t_c estimated by (3), for $S = 1/8$ (red, solid line) and $S = 1/4$ (blue, dashed line). Right: Radial profile of the mean vorticy of the condensate $\Omega(r)$ for $S = 1/8$ (red, solid line) and $S = 1/4$ (blue, dashed line). The scaling behavior $\Omega(r) \sim r^{-1}$ is represented by the black dotted line.

inverse cascade which feeds it, is balanced by the effect of the eddy viscosity at the scale L_x, that is, $\varepsilon_{\rm inv} \simeq \nu_{\rm eddy} E_c / L_x^2$. Using the simple dimensional estimate for the eddy viscosity $\nu_{\rm eddy} \simeq E^{\rm 3D} t_f$ we obtain scaling predictions for the energy of the condensate E_c and the time required to form it $t_c \simeq E_c / \varepsilon_{\rm inv}$:

$$\frac{E_c}{E_f} \simeq \frac{E_f}{E^{\rm 3D}} \left(\frac{L_x}{L_f} \right)^2 \frac{\varepsilon_{\rm inv}}{\varepsilon}; \quad \frac{t_c}{t_f} \simeq \frac{E_f}{E^{\rm 3D}} \left(\frac{L_x}{L_f} \right)^2. \tag{3}$$

Using the values of $\varepsilon_{\rm inv}$ and $E^{\rm 3D}$ measured in the simulations, we get quantitative estimates for E_c and t_c. Rescaling the time and energy with the predictions (3), we observe a good collapse of the temporal evolution of the kinetic energy (see Fig. 4, left panel). The validation of the predictions (3) would require a large set of simulations with different aspect ratios. This is left for future investigations.

In the asymptotic limit of infinite Re and small S, it is possible to derive theoretical scaling predictions for E_c and t_c as a function of the aspect ratios $S = L_z / L_f$ and $r = L_x / L_z$ only. According to the phenomenology described in Ref. [3], three cascade processes take place in the turbulent layer. At large scales ($\ell > L_f$) there is a 2D inverse energy cascade with flux $\varepsilon_{\rm inv}$. At intermediate scales ($L_f > \ell > L_z$) the enstrophy production is negligible, and a 2D direct enstrophy cascade with flux β is observed. At small scales ($\ell < L_z$) the flow becomes 3D and displays a direct energy cascade with flux $\varepsilon_{\rm dir}$, which is assumed to be proportional to the residual flux of energy carried by the enstrophy cascade at the scale L_z, that is, $\varepsilon_{\rm dir} \propto \beta L_z^2$ [3]. Recalling that $\varepsilon_{\rm inv} = \varepsilon - \varepsilon_{\rm dir}$, and that $\varepsilon_{\rm inv} = 0$ for S larger than the critical aspect ratio $S^* = L_z^* / L_f$ [2], one gets $\varepsilon_{\rm inv} / \varepsilon \propto 1 - (S/S^*)^2$. Similarly, one can estimate the energy of the 3D mode as $E^{\rm 3D} \simeq u_z^2$, where u_z is the typical intensity of the velocity at the scale L_z. From the scaling of the direct enstrophy cascade one has $u_z \simeq \beta^{1/3} L_z$, and hence $E^{\rm 3D} \simeq \beta^{2/3} L_z^2 \simeq E_f (L_z / L_f)^2$. Inserting these dimensional estimates in Eq. (3) one obtains the asymptotic scaling predictions:

$$\frac{E_c}{E_f} \simeq \left(\frac{L_x}{L_z} \right)^2 \left[1 - \left(\frac{L_z}{L_z^*} \right)^2 \right], \quad \frac{t_c}{t_f} \simeq \left(\frac{L_x}{L_z} \right)^2. \tag{4}$$

The asymptotic scaling requires a very high Reynolds number to be verified, which cannot be achieved in fully resolved simulations but has been observed in a simplified dynamical model of turbulence [29].
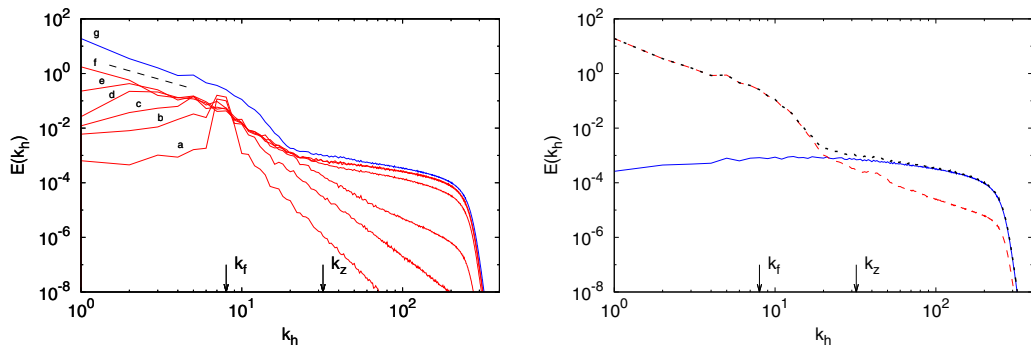
FIG. 5. Left: 2D energy spectra $E(k_h)$ as a function of $k_h = (k_x^2 + k_y^2)^{1/2}$ for $S = 1/4$ at times $t/t_f = 2.4$ (a), 4.8 (b), 7.1 (c), 12 (d), 24 (e), 71 (f), and 2650 (g). The black dashed line represents the scaling $k^{-5/3}$. Right: 2D energy spectrum $E(k_h)$ as a function of $k_h = (k_x^2 + k_y^2)^{1/2}$ of the 2D mode $\boldsymbol{u}^{2D}$ (red, dashed line), 3D mode $\boldsymbol{u}^{3D}$ (blue, solid line), and total velocity field $\boldsymbol{u}$ (black, dotted line) as a function of the horizontal wave number k_h.

Following Ref. [23], we have computed the mean 2D vorticity field of the condensate, as the temporal average in the stationary regime of the fields ω_z, which have been previously averaged in the vertical direction z and then centered on the position of the center of mass of the vorticity. The radial vorticity profile of the condensate $\Omega(r)$ (shown in Fig. 4, right panel) is characterized by a vortex core (for $r < R_c$) in which the vorticity is almost constant, as in solid body rotation. Rescaling the radial distance with a dimensional estimate for the radius of the core $R_c \simeq \sqrt{E/Z}$, where $Z = (1/2)\langle |\boldsymbol{\omega}|^2 \rangle$ is the enstrophy, we observe a good collapse of the core (see inset of Fig. 4, right panel). The radius R_c represents the scale at which the centripetal force of the vortex is balanced by the inertial forces of turbulence.

Outside the core we observe for the case $S = 1/4$, a power-law behavior for the vorticity profile $\Omega(r) \sim r^{-1}$, which is suggestive of a similar observation in 2D turbulence [23]. However, in Ref. [23] this scaling is derived from the balance with a friction force which is not present in our 3D case. Different predictions has been derived for a 2D viscous condensate [30]. In both cases [23,30] the 2D scalings are expected for scales $r > L_f$ while in our simulation the scaling range is $R_c < r < L_f$. Further investigations are required to achieve a better understanding of the profile of the 3D condensate and its relations with the 2D case.

In Fig. 5 we show the 2D energy spectra for the case $S = 1/4$, defined as

$$E(k_h) = \frac{1}{2} \sum_{\substack{\boldsymbol{k} \\ k_x^2 + k_y^2 = k_h^2}} |\hat{\boldsymbol{u}}_{\boldsymbol{k}}|^2, \tag{5}$$

where $k_h = (k_1^2 + k_2^2)^{1/2}$ is the horizontal wave number. At short time the spectra shows the development of the inverse energy cascade for $k_h > k_f$ with a $-5/3$ spectral slope. At late times, the spectrum of the steady condensed state contains much more energy than the spectrum of the inverse cascade in a broad wave-number range ($k_h > k_z$). In the range $k_h > k_f$ the spectral slope is close to -2. A similar spectral behavior is observed for the case $S = 1/8$ (not shown).

In order to highlight the different contributions of the 2D and 3D modes to the spectrum of the condensate, we show in Fig. 5 the 2D energy spectra of the fields $\boldsymbol{u}^{2D}$ and $\boldsymbol{u}^{3D}$. The energy of the 2D mode is dominant for $k_h > k_z$, which confirms the two-dimensional nature of the condensed state. Conversely, the 3D mode becomes dominant at small scales $k_h > k_z$.
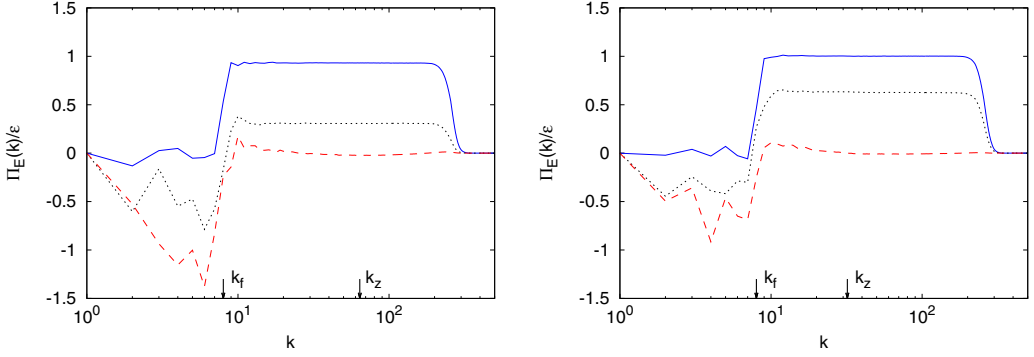
FIG. 6. Left: Spectral energy flux $\Pi(k)$ for $S = 1/8$ at time $t = 25t_f$ (black, dotted line), $t = 4050t_f$ (blue, solid line), and 2D energy flux $\Pi^{2D}(k)$ at $t = 4050t_f$ (red, dashed line). Right: Spectral energy flux $\Pi(k)$ for $S = 1/4$ at time $t = 25t_f$ (black, dotted line), $t = 2650t_f$ (blue, solid line), and 2D energy flux $\Pi^{2D}(k)$ at $t = 2650t_f$ (red, dashed line).

The spectral energy flux, defined as

$$\Pi(k) = -\frac{1}{2} \sum_{\substack{\boldsymbol{k}, \boldsymbol{p}, \boldsymbol{q} \\ |\boldsymbol{k}| \leqslant k \\ \boldsymbol{k} + \boldsymbol{p} + \boldsymbol{q} = 0}} \hat{\boldsymbol{u}}_{\boldsymbol{k}}^* \cdot (i\boldsymbol{k} \cdot \hat{\boldsymbol{u}}_{\boldsymbol{p}})\hat{\boldsymbol{u}}_{\boldsymbol{q}} + \text{c.c.} \tag{6}$$

gives further information concerning the mechanisms of the formation and saturation of the condensate. In the early stage in which the condensate grows ($t = 25t_f$ in Fig. 6), the energy flux shows clearly the splitting of the energy cascade (as in Refs. [2,3]). A fraction of the energy is transported toward small wave numbers $k < k_f$ with a negative flux ε_{inv}, while the remnant energy performs a direct cascade toward large k with flux ε_{dir}. In the late stage ($t = 2650t_f$ in Fig. 6) when the condensate has reached a steady state, the average flux is zero for $k < k_f$ and is equal to the energy input ε for $k > k_f$. Nonetheless, the flux of the 2D mode transported by the 2D velocity $\Pi^{2D}(k)$ [defined as in Eq. (6) but restricting the fields to $\boldsymbol{u}^{2D}$] reveals that also at late times, there is a negative flux of 2D energy at $k < k_f$. Therefore the condensate is still fed by a 2D inverse energy cascade. The negative energy flux, which proceeds from the forcing scale to the scale of the condensate, is exactly balanced by an opposite energy transfer from the condensate to the small-scale 3D flow.

To investigate the interactions between the 2D and 3D modes at different scales, we partition the Fourier space in nonoverlapping spherical shells $n\Delta K \leqslant |\boldsymbol{k}| < (n+1)\Delta K$, labeled with $K = 1 + n\Delta K$, with $\Delta K = 4$. Then, we decompose the velocity field as $\boldsymbol{u} = \sum_K \boldsymbol{u}_K$, where $\boldsymbol{u}_K$ is the velocity field filtered in the shell K. Following [31] we define the rate of energy transfer $T(K, Q)$ from the shell Q to the shell K as

$$T(K, Q) = -\sum_P \int d\boldsymbol{x}^3 \boldsymbol{u}_K \cdot (\boldsymbol{u}_P \cdot \boldsymbol{\nabla})\boldsymbol{u}_Q. \tag{7}$$

Similarly, we define the 2D transfer $T^{2D}(K, Q)$ in terms of the filtered 2D modes $\boldsymbol{u}_K^{2D}$. In Fig. 7 we plot the spectral energy transfer toward the shell $K = 1$ which contains the condensate. In order to reduce the statistical fluctuations, we have averaged $T(K, Q)$ and $T^{2D}(K, Q)$ for times larger than the time t_s required to reach the statistical steady state. In both cases $S = 1/4$ and $S = 1/8$ we observe that the shells with $Q < k_z$ give positive contributions to the condensate. In this range of wave numbers, the 2D transfer $T^{2D}(K, Q)$ coincides with the total transfer $T(K, Q)$, showing that the condensate is fed solely by the interactions between large-scale 2D modes. Conversely, the
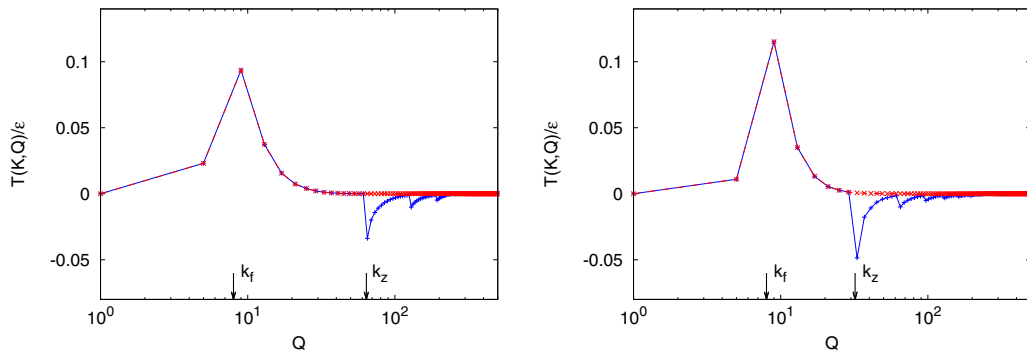
FIG. 7. Spectral energy transfer $T(K, Q)$ (blue, crosses), and 2D spectral energy transfer $T^{2D}(K, Q)$ (red, times) for $K = 1$, averaged in time for $t > t_s$. Left panel: $S = 1/8$, $t_s = 3000t_f$. Right panel: $S = 1/4$, $t_s = 2500t_f$.

modes $Q \geqslant k_z$ take away energy from the condensate, but their negative contributions to $T(K, Q)$ are canceled out in $T^{2D}(K, Q)$. This demonstrates that the condensate reaches a statistical steady state because of interactions with the small-scale 3D modes which subtract energy from it. The nonlocal nature of these interactions is evident, because they occur between the shell $K = 1$ and the modes $Q \geqslant k_z \gg 1$.

In conclusion, we have shown that by confining the turbulent flow, forced at small scale L_f, in a thin fluid layer, it is possible to observe the formation of a statistically steady condensed state, which has the form of a quasi-two-dimensional dipole. By means of direct numerical simulations we have analyzed the temporal evolution of the kinetic energy and its spectral distribution, showing that the condensate is composed mainly by the 2D mode. We have also demonstrated that the saturation of the energy of the condensate is due to the balance of two processes: an inverse cascade of 2D energy, which proceeds from the forcing scale toward the large scales $\ell > L_f$, and a direct energy transfer from the condensate toward the 3D turbulent flow at small scales $\ell < L_z$. The latter process is similar to the viscous dissipative process which arrests the cascade in a purely 2D flow, but the role of the viscosity is here replaced by the eddy viscosity of the 3D flow.

It is worth remarking that, because of the dissipative anomaly, the eddy viscosity does not vanish in the limit $\nu \to 0$. This guarantees the saturation of the energy to a finite value also in the limit of Re $\to \infty$. This result is of particular interest for geophysical applications, in which the vertical scale L_z of the fluid layers is much larger than the viscous scales. In view of possible application of our findings to more realistic geophysical situations, it would be extremely interesting to investigate the problem with different boundary conditions and how the presence of the Coriolis force and of a stable stratification of density affects the formation of the condensate and its saturation.

---

[1] L. M. Smith, J. R. Chasnov, and F. Waleffe, Crossover from Two- to Three-Dimensional Turbulence, Phys. Rev. Lett. **77**, 2467 (1996).

[2] A. Celani, S. Musacchio, and D. Vincenzi, Turbulence in More than Two and Less than Three Dimensions, Phys. Rev. Lett. **104**, 184506 (2010).

[3] S. Musacchio and G. Boffetta, Split energy cascade in turbulent thin fluid layers, Phys. Fluids **29**, 111106 (2017).

[4] A. Alexakis and L. Biferale, Cascades and transitions in turbulent flows, Phys. Rep. **767-769**, 1 (2018).

[5] M. Shats, D. Byrne, and H. Xia, Turbulence Decay Rate as a Measure of Flow Dimensionality, Phys. Rev. Lett. **105**, 264501 (2010).

[6] D. Byrne, H. Xia, and M. Shats, Robust inverse energy cascade and turbulence structure in three-dimensional layers of fluid, Phys. Fluids **23**, 095109 (2011).

[7] H. Xia, D. Byrne, G. Falkovich, and M. Shats, Upscale energy transfer in thick turbulent fluid layers, Nat. Phys. **7**, 321 (2011).

[8] H. Xia and N. Francois, Two-dimensional turbulence in three-dimensional flows, Phys. Fluids **29**, 111107 (2017).

[9] S. J. Benavides and A. Alexakis, Critical transitions in thin layer turbulence, J. Fluid Mech. **822**, 364 (2017).

[10] L. M. Smith and F. Waleffe, Transfer of energy to two-dimensional large scales in forced, rotating three-dimensional turbulence, Phys. Fluids **11**, 1608 (1999).

[11] E. Lindborg, The effect of rotation on the mesoscale energy cascade in the free atmosphere, Geophys. Res. Lett. **32**, L01809 (2005).

[12] E. Deusebio, G. Boffetta, E. Lindborg, and S. Musacchio, Dimensional transition in rotating turbulence, Phys. Rev. E **90**, 023005 (2014).

[13] A. Pouquet, R. Marino, P. D. Mininni, and D. Rosenberg, Dual constant-flux energy cascades to both large scales and small scales, Phys. Fluids **29**, 111108 (2017).

[14] G. Brethouwer, P. Billant, E. Lindborg, and J.-M. Chomaz, Scaling analysis and simulation of strongly stratified turbulent flows, J. Fluid Mech. **585**, 343 (2007).

[15] A. Sozza, G. Boffetta, P. Muratore-Ginanneschi, and S. Musacchio, Dimensional transition of energy cascades in stably stratified forced thin fluid layers, Phys. Fluids **27**, 035112 (2015).

[16] M. Hossain, William H. Matthaeus, and D. Montgomery, Long-time states of inverse cascades in the presence of a maximum length scale, J. Plasma Phys. **30**, 479 (1983).

[17] L. M. Smith and V. Yakhot, Bose Condensation and Small-Scale Structure Generation in a Random Force Driven 2D Turbulence, Phys. Rev. Lett. **71**, 352 (1993).

[18] J. Sommeria, Experimental study of the two-dimensional inverse energy cascade in a square box, J. Fluid Mech. **170**, 139 (1986).

[19] H. Xia, H. Punzmann, G. Falkovich, and M. G. Shats, Turbulence-Condensate Interaction in Two Dimensions, Phys. Rev. Lett. **101**, 194504 (2008).

[20] H. Xia, M. Shats, and G. Falkovich, Spectrally condensed turbulence in thin layers, Phys. Fluids **21**, 125101 (2009).

[21] M. Chertkov, C. Connaughton, I. Kolokolov, and V. Lebedev, Dynamics of Energy Condensation in Two-Dimensional Turbulence, Phys. Rev. Lett. **99**, 084501 (2007).

[22] B. Gallet and W. R. Young, A two-dimensional vortex condensate at high Reynolds number, J. Fluid Mech. **715**, 359 (2013).

[23] J. Laurie, G. Boffetta, G. Falkovich, I. Kolokolov, and V. Lebedev, Universal Profile of the Vortex Condensate in Two-Dimensional Turbulence, Phys. Rev. Lett. **113**, 254503 (2014).

[24] A. Frishman and C. Herbert, Turbulence Statistics in a Two-Dimensional Vortex Condensate, Phys. Rev. Lett. **120**, 204505 (2018).

[25] A. Frishman, J. Laurie, and G. Falkovich, Jets or vortices-What flows are generated by an inverse turbulent cascade? Phys. Rev. Fluids **2**, 032602 (2017).

[26] F. Bouchet and E. Simonnet, Random Changes of Flow Topology in Two-Dimensional and Geophysical Turbulence, Phys. Rev. Lett. **102**, 094504 (2009).

[27] G. L. Eyink, Exact results on stationary turbulence in 2D: Consequences of vorticity conservation, Physica D **91**, 97 (1996).

[28] G. Boffetta and R. E. Ecke, Two-dimensional turbulence, Annu. Rev. Fluid Mech. **44**, 427 (2012).

[29] G. Boffetta, F. De Lillo, and S. Musacchio, Shell model for quasi-two-dimensional turbulence, Phys. Rev. E **83**, 066302 (2011).

[30] I. V. Kolokolov and V. V. Lebedev, Profile of coherent vortices in two-dimensional turbulence, JETP Lett. **101**, 164 (2015).

[31] A. Alexakis, P. D. Mininni, and A. Pouquet, Imprint of Large-Scale Flows on Turbulence, Phys. Rev. Lett. **95**, 264503 (2005).